Acta Crystallographica Section C
Crystal Structure Communications
ISSN 0108-2701

Two- and three-dimensional hydrated coordination polymers of diaqua-lanthanum(3+) ions with 2-hydroxypropanedioate, oxalate and acetate anions as bridging ligands

Rajesh Koner and Israel Goldberg*

School of Chemistry, Sackler Faculty of Exact Sciences, Tel-Aviv University, Ramat-Aviv, 69978 Tel-Aviv, Israel
Correspondence e-mail: goldberg@post.tau.ac.il

Received 12 February 2009
Accepted 10 March 2009
Online 21 March 2009

The title compounds, poly[[tetraaquadi-μ-2-hydroxypropanedioato-μ-oxalato-dilanthanum(III)] tetrahydrate], $\{[La_2(C_2O_4)(C_3H_2O_5)_2(H_2O)_4]\cdot 4H_2O\}_n$, (I), and poly[[tetra-$\mu$-acetato-tetraaqua-$\mu$-oxalato-dilanthanum(III)] dihydrate], $\{[La_2(C_2O_4)(C_2H_3O_2)_4(H_2O)_4]\cdot 2H_2O\}_n$, (II), represent crystalline hydrates of coordination polymers of diaqualanthanum(3+) ions with different combinations of bridging carboxylate ligands, *viz*. 2-hydroxypropanedioate and oxalate in a 2:2:1 ratio in (I), and acetate and oxalate in a 2:4:1 ratio in (II). While the acetate component was one of the reactants used, the other ligands were obtained *in situ* by aerial oxidation of the dihydroxyfumaric acid present in the reactions. The crystal structure of (I) consists of two-dimensional polymeric arrays with water molecules intercalated between and hydrogen bonded to the arrays. The oxalate components are located on inversion centres. The crystal structure of (II) reveals an open three-dimensional polymeric connectivity between the interacting components, with the solvent water molecules incorporated within the intralattice voids and hydrogen bonded to the polymeric framework. The La^{III} ion and the noncoordinated water molecules are located on axes of twofold symmetry. The oxalate group is centred at the 222 symmetry site, the intersection of the three rotation axes. The coordination number of the La^{III} ion in the two structures is 10. The significance of this study lies mainly in the characterization of two new coordination polymers, as well as in the confirmation that dihydroxyfumaric acid tends to rearrange to form smaller components in standard laboratory procedures, and should be considered a poor reagent for formulating hybrid coordination polymers with metal ions.

Comment

This report is part of a broad study related to the formulation of extended coordination polymers by reacting lanthanide metal ions with organic polycarboxylic acids as chelating ligands (George *et al.*, 2006; Lipstman *et al.*, 2007; Muniappan *et al.*, 2007; Koner & Goldberg, 2008). The latter may link simultaneously to metal centres in a variety of coordination modes and thus generate extended coordination networks and frameworks. The lanthanide ions provide a very attractive interface to promote the formation of such polymeric arrays due to their large size, spatial divergence of the valent orbitals, high coordination numbers and (due to their 'hard' nature) high affinity for oxo ligands. Moreover, deprotonated carboxylate ligands also act as counter-ions to balance the charge. The high propensity of the lanthanides to form multicomponent structures with acetate, oxalate and other small carboxylate anions is well documented in the Cambridge Structural Database (CSD; Version 5.30 of November 2008; Allen, 2002). Their reaction with more bulky tetra(carboxyphenyl)porphyrin ligands has led to the formulation of robust microporous solids (George *et al.*, 2006; Lipstman *et al.*, 2007; Muniappan *et al.*, 2007). Examples of coordination networks formed by the reaction of first-row transition metals with polycarboxylic acid ligands are also known (*e.g.* Abrahams *et al.*, 2006; Goldberg, 2005).

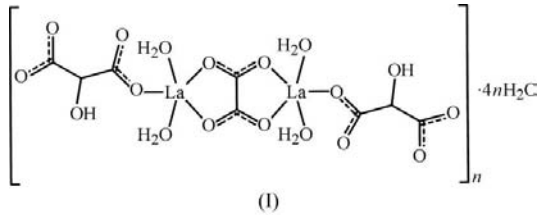

(I)

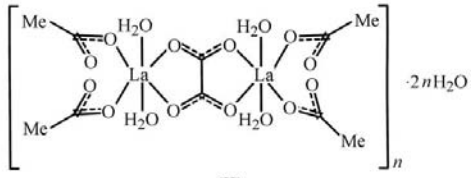

(II)

In the above context, we reacted a lanthanum nitrate salt with the dicarboxylic acid dihydroxyfumaric acid in the presence of sodium acetate, aiming to explore the capacity of the multidentate fumaric acid moiety to induce the formation of extended coordination polymers under different conditions. However, in the experiments we performed and in the presence of the lanthanum metal ions, the dihydroxyfumaric acid decomposed to 2-hydroxypropanedioate and oxalate anions *via* a metal-promoted benzylic acid-type rearrangement (Selman & Eastman, 1960). Similar aerial oxidation reactions of dihydroxyfumaric acid to smaller components have been reported in earlier studies with first-row transition metals (Abrahams *et al.*, 2006, 2004). Thus, with the ligands generated *in situ*, coordination polymers of the following stoichiometric composition have been obtained and structurally characterized: $[La(H_2O)_2(OOCCHOHCOO)(OOCCOO)_{0.5}]\cdot 2H_2O$, (I), and $[La(H_2O)_2(CH_3COO)_2(OOCCOO)_{0.5}]\cdot H_2O$, (II). Representations of the two structures are shown in Figs. 1 and 2, respectively.

Structure (I) can be best described as composed of two-dimensional coordination networks between the component

  doi:10.1107/S0108270109008798

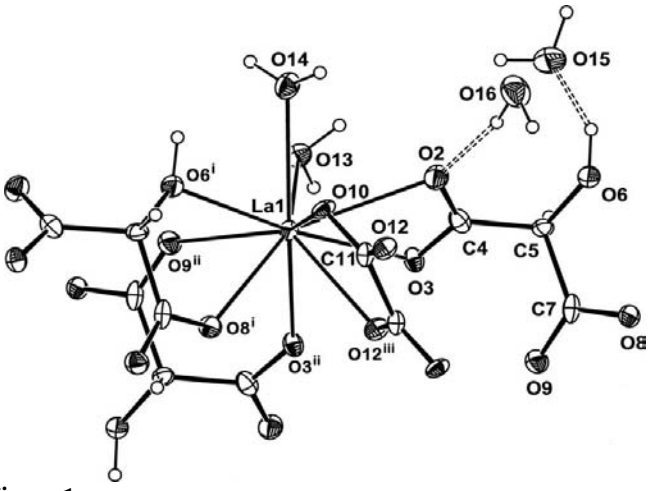

Figure 1
The coordination environment of the La^{III} ion in (I), showing the atom-labelling scheme. Displacement ellipsoids are drawn at the 50% probability level at 110 (2) K and H atoms are shown as small spheres of arbitrary radii. Hydrogen bonds to the noncoordinated water molecules are indicated by dashed lines. The oxalate ligand is located on a crystallographic inversion centre at ($\frac{1}{2}$, 0, 0). [Symmetry codes: (i) $x-\frac{1}{2}, \frac{1}{2}-y, z-\frac{1}{2}$; (ii) $1-x, 1-y, -z$; (iii) $1-x, -y, -z$.]

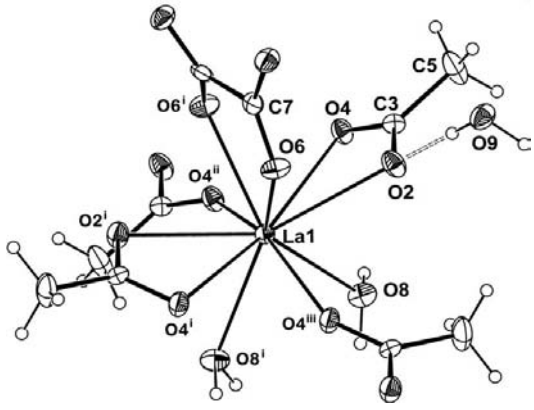

Figure 2
The coordination environment of the La^{III} ion in (II), showing the atom-labelling scheme. Displacement ellipsoids are drawn at the 50% probability level at 110 (2) K and H atoms are shown as small spheres of arbitrary radii. The hydrogen bond to the noncoordinated water molecule is indicated by a dashed line. The La^{III} ions are located on a twofold rotation axis at ($\frac{5}{8}$, $\frac{1}{8}$, z). The centre of the oxalate anion coincides with the 222 symmetry site at ($\frac{5}{8}$, $\frac{1}{8}$, $\frac{1}{8}$). The noncoordinated O9 water molecule is located on a twofold rotation axis at ($\frac{3}{8}$, $\frac{3}{8}$, z). [Symmetry codes: (i) $\frac{5}{4}-x, \frac{1}{4}-y, z$; (ii) $1-x, -y, -z$; (iii) $x+\frac{1}{4}, y+\frac{1}{4}, -z$.]

species. As shown in Fig. 3, the La^{III} ion exhibits multiple binding modes to the surrounding species. It is coordinated by three hydroxymalonate units, involving both their carboxylate and hydroxyl sites. Two additional ligating sites are associated with the carboxylate groups of the oxalate anion. The coordination environment of the La^{III} ion is supplemented by two molecules of water, O13 and O14, which are oriented outward, above and below and roughly perpendicular to the surface of the coordination network. The coordination number of the La^{III} ions is essentially 10, with the La—O bond distances varying from 2.494 (4) to 2.758 (4) Å (Table 1). Each of the multidentate 2-hydroxypropanedioate ligands coordinates

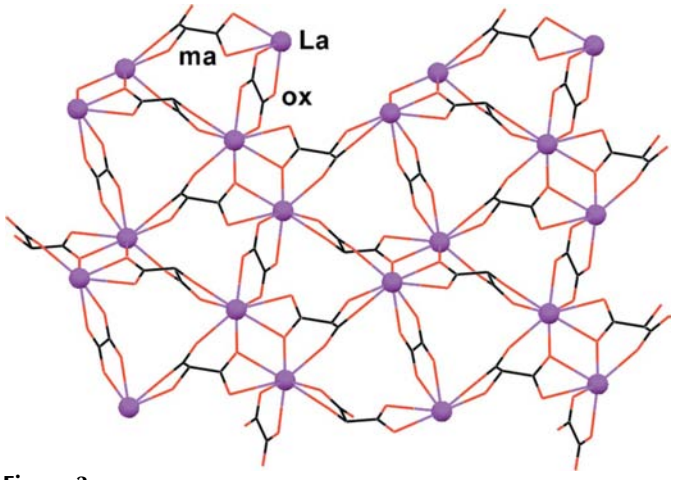

Figure 3
Wireframe illustration of the two-dimensional supramolecular coordination scheme in (I), with the La^{III} ions denoted by spheres. The malonate and oxalate species are labelled 'ma' and 'ox', respectively. The two coordinated water ligands, O13 and O14, oriented perpendicular to the coordination network, have been omitted for clarity.

simultaneously to three metal centres, while the bis-bidentate oxalate ligand (with four carboxylate O-atom sites) bridges two neighbouring metal ions. This extensive crosslinking yields a robust coordination network, aligned in the crystal structure approximately normal to the [$\bar{2}$01] direction. The polymeric layers are stacked in a parallel manner along the normal direction, intercalating molecules of noncoordinated solvent water (O15 and O16) between them (Fig. 4). These water species provide an extensive O—H···O hydrogen-bonding connection scheme between neighbouring polymeric arrays (Table 2), yielding a fully interlinked intermolecular organization.

The structure of (II) represents a three-dimensional coordination polymer. This compound was prepared under harsher conditions than compound (I), *viz.* an overnight reflux at elevated temperature compared with simple stirring of the reaction mixture at room temperature. This resulted in

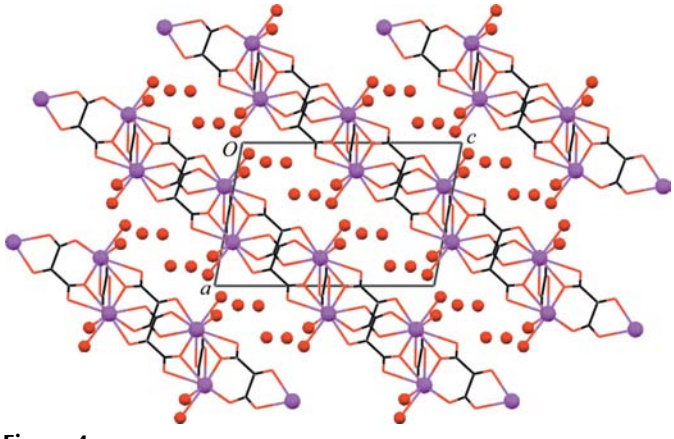

Figure 4
The crystal structure of (I), projected down the *b* axis, showing four neighbouring coordination networks edge-on. The La^{III} ions and all the coordinated and noncoordinated water molecules are denoted by spheres.

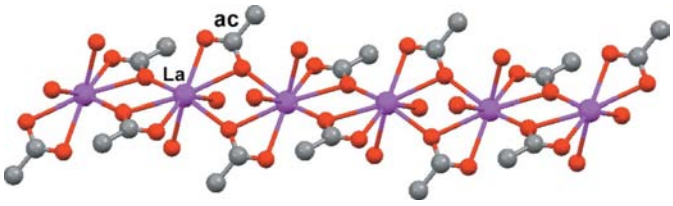

Figure 5
Ball-and-stick illustration of the intercoordination of the La^{III} ions through the acetate ligands into polymeric chain arrays in (II). H atoms have been omitted for clarity. The acetate species is labelled 'ac'. The sideways coordination to the oxalate ligands is not shown; these chains run along the [110] and [1$\bar{1}$0] directions.

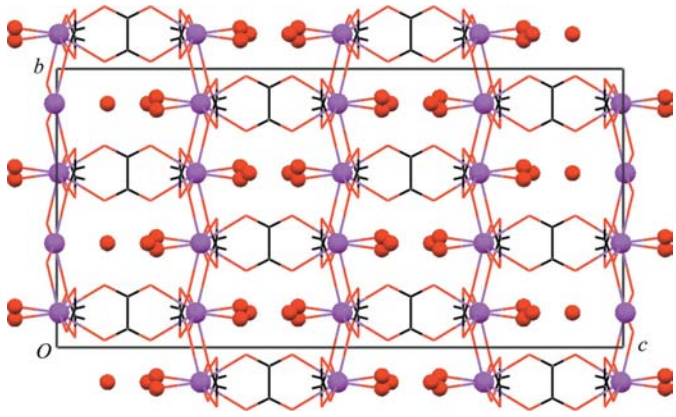

Figure 6
The crystal structure of (II), viewed down the *a* axis. The La^{III} ions and all water molecules are denoted by spheres. H atoms have been omitted. Note the nearly perpendicular orientation of the acetate and oxalate ligands, which facilitates the three-dimensional connectivity of the component species into a single-framework coordination polymer.

incorporation of the acetate anions into the coordination environment of the metal and elimination of possible coordination of the hydroxymalonic species, as in (I). A modular description of the observed coordination networking follows.

The La^{III} ions of (II) are assembled into polymeric chains by the bridging acetate ligands, with two acetate moieties connecting between each pair of neighbouring diaquametal ions (Fig. 5 and Table 3). Such coordination has been observed previously with the acetate ligand (Dan *et al.*, 2006), as well as with a number of other monocarboxylate entities (CSD; 26 hits). These chains are oriented perpendicular to the *c* axis, being centred at the *z*-coordinated levels of 0, $\frac{1}{4}$, $\frac{1}{2}$ and $\frac{3}{4}$. Chains located at $z = 0$ and $z = \frac{1}{2}$ propagate along [110], while those located at $z = \frac{1}{4}$ and $z = \frac{3}{4}$ are aligned along [1$\bar{1}$0]. The periphery of these chains is decorated by the lipophilic methyl groups. At each *z*-coordinate level, neighbouring chains are related to one another by translation along either [1$\bar{1}$0] (at $z = 0$ and $\frac{1}{2}$) or [110] (at $z = \frac{1}{4}$ and $\frac{3}{4}$). They are interlinked by O—H···O hydrogen bonding through the noncoordinated water solvent molecule (Table 4), thus forming layers parallel to the *ab* plane. These chains, and thus the layers, at different *z* levels are intercoordinated further by oxalate ligands in the *c* direction. A given chain at one *z* level (*e.g.* at $z = \frac{1}{2}$) is linked simultaneously to different (perpendicularly oriented) chains at the neighbouring *z* levels (at $z = \frac{1}{4}$ and $z = \frac{3}{4}$), thus yielding a unique three-dimensional coordination framework. Hence, coordination between the La^{III} ions through the acetate ligands, along with hydrogen bonding between the polymeric chains thus formed, forms layers parallel to (001), while additional multiple coordination between the metal ions through the oxalate ligands connects these layers along [001].

A view of the crystal structure of (II) is shown in Fig. 6. It illustrates the layered arrangement of the acetate-bridged polymeric chains, which extend parallel to the *ab* plane at equal intervals along the *c* axis, and the effective bridging between these layers along *c* by the oxalate 'pillars'. Similar polymeric coordination modes of lanthanide oxalates have been reported previously (*e.g.* Song & Mao, 2005). However, to the best of our knowledge, structures of polymeric arrays involving a combination of acetate and oxalate ligands in the same compound have not been reported to date.

The La—O coordination bonds in (II) are within the range 2.524 (2)–2.748 (2) Å (Table 3). The observed coordination number of the metal ion is 10 in (I) and (II), although the 3+ lanthanides most commonly exhibit coordination numbers up to 9 (Muniappan *et al.*, 2007; Lipstman *et al.*, 2007). This observation can be associated with the bifurcated nature of the carboxylate binding, and the occurrence of somewhat elongated (>2.6 Å) La—O bonds. A survey of the CSD involving 3436 hits from crystal structures with $R < 0.05$ reveals that previously reported La—O bond lengths range from 2.136 to 3.224 Å, with a mean distance of 2.57 (12) Å. The La—O distance ranges observed in (I) and (II) are thus in agreement with the previously reported data.

In summary, this study reports two new metal–ligand coordination polymers involving La^{III} ions and small carboxylate ligands. They were found to reveal unique coordination connectivities, expanding on the known structural variety involving lanthanide metal ions. The diverse coordination capacity of these ions may justify further research in this area.

Experimental

All reactants and solvents were obtained commercially. For both compounds, an aqueous solution (25 ml) of $La(NO_3)_3{\cdot}6H_2O$ (0.433 g, 1 mmol) was added dropwise to a suspension containing dihydroxyfumaric acid (0.092 g, 0.05 mmol) and sodium acetate trihydrate (0.136 g, 1 mmol) in H_2O (25 ml). For compound (I), the mixture was stirred overnight at room temperature. It was then filtered and the filtrate was kept undisturbed for several days, yielding light-yellow diffraction quality single crystals of (I). IR (KBr, ν, cm^{-1}): 3200–3455 (broad strong band, can be assigned as water stretching), 1632 (*s*, ν_{as} of COO^-), 1364 (ν_s of COO^-), 2905 (*w*), 794 (*m*) and 690 (*m*) (C—H). For compound (II), the mixture of reactants described above was refluxed overnight, filtered and left to crystallize under ambient conditions, yielding X-ray quality crystals of (II). IR (KBr, cm^{-1}): broad band centred at around 3448 can be assigned as due to water stretching, 1674 and 1625 (ν_{as} of OCO^-), 1349 and 1300 (ν_s of OCO^-), 800 [δ(OCO, bis-bidentate oxalate)], 1591 (*s*, acetate stretching).

Compound (I)

Crystal data

$[La_2(C_2O_4)(C_3H_2O_5)_2(H_2O)_4]\cdot 4H_2O$
M_r = 746.06
Monoclinic, $P2_1/n$
a = 9.1139 (2) Å
b = 8.3883 (2) Å
c = 13.6994 (4) Å
β = 100.9688 (10)°
V = 1028.19 (4) Å^3
Z = 2
Mo $K\alpha$ radiation
μ = 4.21 mm^{-1}
T = 110 K
0.20 × 0.15 × 0.07 mm

Data collection

Nonius KappaCCD area-detector diffractometer
Absorption correction: multi-scan (Blessing, 1995)
T_{min} = 0.487, T_{max} = 0.757
9704 measured reflections
2481 independent reflections
1950 reflections with $I > 2\sigma(I)$
R_{int} = 0.059

Refinement

$R[F^2 > 2\sigma(F^2)]$ = 0.037
$wR(F^2)$ = 0.098
S = 1.00
2481 reflections
145 parameters
H-atom parameters constrained
$\Delta\rho_{max}$ = 2.55 e Å^{-3}
$\Delta\rho_{min}$ = −1.13 e Å^{-3}

Compound (II)

Crystal data

$[La_2(C_2O_4)(C_2H_3O_2)_4(H_2O)_4]\cdot 2H_2O$
M_r = 710.12
Orthorhombic, *Fddd*
a = 12.1763 (2) Å
b = 13.3596 (2) Å
c = 27.2064 (6) Å
V = 4425.68 (14) Å^3
Z = 8
Mo $K\alpha$ radiation
μ = 3.89 mm^{-1}
T = 110 K
0.35 × 0.30 × 0.15 mm

Data collection

Nonius KappaCCD area-detector diffractometer
Absorption correction: multi-scan (Blessing, 1995)
T_{min} = 0.343, T_{max} = 0.593
(expected range = 0.323–0.558)
7496 measured reflections
1320 independent reflections
1112 reflections with $I > 2\sigma(I)$
R_{int} = 0.042

Refinement

$R[F^2 > 2\sigma(F^2)]$ = 0.028
$wR(F^2)$ = 0.066
S = 1.38
1320 reflections
74 parameters
H-atom parameters constrained
$\Delta\rho_{max}$ = 2.66 e Å^{-3}
$\Delta\rho_{min}$ = −1.07 e Å^{-3}

H atoms bound to C atoms were located in calculated positions and constrained to ride on their parent atoms, with the following parameters: for (I), Csp^3—H = 1.00 Å (relates to a tertiary C atom) and U_{iso}(H) = 1.2U_{eq}(C); for (II), Csp^3—H = 0.98 Å (relates to a terminal methyl group) and U_{iso}(H) = 1.5U_{eq}(C). H atoms bound to O atoms were either located in difference Fourier maps or positioned to optimize intermolecular hydrogen bonding. All O—H bond lengths were first restrained to 0.90 (2) Å, but then kept fixed in the final least-squares cycles. In (I), these H atoms were assigned U_{iso}(H) = 1.2U_{eq}(O), while in (II) their U_{iso}(H) values were refined in an unconstrained manner. Significant residual electron-density peaks were observed in (I) in the vicinity of the O14 water ligand: a single peak of 2.5 e Å^{-3} at 1.3 Å from O14 and two peaks of 1.4 e Å^{-3} at 2.8–2.9 Å from O14. They may represent an unidentified disorder of this ligand and the possible presence of additional proximal water molecule(s) with partial occupancy. Similarly, a single residual electron-density peak of 2.7 e Å^{-3} (the remaining residual peaks are below 0.55 e Å^{-3}) located on a twofold axis at ($\frac{1}{8}$, $\frac{1}{8}$, −0.007) was found in (II). It could not be accounted for, possibly resulting from a ripple of the Fourier map on a symmetry element due to the presence of the heavy atom.

Table 1
Selected bond lengths (Å) for (I).

La1—O2	2.758 (4)	La1—O9^{i}	2.560 (4)
La1—O3	2.671 (3)	La1—O10	2.589 (4)
La1—O3^{i}	2.494 (4)	La1—O12^{iii}	2.592 (4)
La1—O6^{ii}	2.581 (4)	La1—O13	2.662 (4)
La1—O8^{ii}	2.530 (4)	La1—O14	2.596 (4)

Symmetry codes: (i) $-x+1, -y+1, -z$; (ii) $x-\frac{1}{2}, -y+\frac{1}{2}, z-\frac{1}{2}$; (iii) $-x+1, -y, -z$.

Table 2
Hydrogen-bond geometry (Å, °) for (I).

D—H···A	D—H	H···A	D···A	D—H···A
O6—H6···O15	0.90	1.84	2.625 (6)	145
O13—H13A···O12^{iv}	0.90	1.92	2.795 (5)	164
O13—H13B···O16^{v}	0.90	1.88	2.739 (6)	158
O14—H14A···O13^{vi}	0.90	1.91	2.785 (5)	163
O14—H14B···O15^{vii}	0.90	2.00	2.871 (6)	162
O15—H15A···O10^{v}	0.90	1.88	2.733 (6)	156
O15—H15B···O16^{v}	0.90	1.95	2.746 (6)	146
O16—H16A···O9^{viii}	0.90	2.24	2.952 (6)	136
O16—H16B···O2	0.90	1.85	2.736 (6)	166

Symmetry codes: (iv) $x, y+1, z$; (v) $-x+\frac{1}{2}, y+\frac{1}{2}, -z+\frac{1}{2}$; (vi) $-x, -y+1, -z$; (vii) $-x+\frac{1}{2}, y-\frac{1}{2}, -z+\frac{1}{2}$; (viii) $-x+\frac{3}{2}, y-\frac{1}{2}, -z+\frac{1}{2}$.

Table 3
Selected bond lengths (Å) for (II).

La1—O2	2.655 (2)	La1—O6	2.566 (3)
La1—O4	2.748 (2)	La1—O8	2.587 (3)
La1—O4^{i}	2.524 (2)		

Symmetry code: (i) $-x+1, -y, -z$.

Table 4
Hydrogen-bond geometry (Å, °) for (II).

D—H···A	D—H	H···A	D···A	D—H···A
O8—H8A···O6^{ii}	0.88	1.85	2.720 (4)	170
O8—H8B···O9^{iii}	0.91	1.93	2.781 (4)	156
O9—H9···O2	0.90	1.87	2.764 (3)	176

Symmetry codes: (ii) $x-\frac{1}{4}, y-\frac{1}{4}, -z$; (iii) $-x+1, y-\frac{1}{4}, z-\frac{1}{4}$.

For both compounds, data collection: *COLLECT* (Nonius, 1999); cell refinement: *DENZO* (Otwinowski & Minor, 1997); data reduction: *DENZO*; program(s) used to solve structure: *SIR97* (Altomare *et al.*, 1999); program(s) used to refine structure: *SHELXL97* (Sheldrick, 2008); molecular graphics: *ORTEPIII* (Burnett & Johnson, 1996) and *Mercury* (Macrae *et al.*, 2006); software used to prepare material for publication: *SHELXL97*.

This research was supported in part by the Israel Science Foundation (grant No. 502/08).

Supplementary data for this paper are available from the IUCr electronic archives (Reference: GT3003). Services for accessing these data are described at the back of the journal.

References

Abrahams, B. F., Hudson, T. A. & Robson, R. (2004). *J. Am. Chem. Soc.* **126**, 8624–8625.
Abrahams, B. F., Hudson, T. A. & Robson, R. (2006). *J. Mol. Struct.* **796**, 2–8.
Allen, F. H. (2002). *Acta Cryst.* B**58**, 380–388.
Altomare, A., Burla, M. C., Camalli, M., Cascarano, G. L., Giacovazzo, C., Guagliardi, A., Moliterni, A. G. G., Polidori, G. & Spagna, R. (1999). *J. Appl. Cryst.* **32**, 115–119.
Blessing, R. H. (1995). *Acta Cryst.* A**51**, 33–38.
Burnett, M. N. & Johnson, C. K. (1996). *ORTEPIII*. Report ORNL-6895. Oak Ridge National Laboratory, Tennessee, USA.
Dan, M., Cheetham, A. K. & Rao, C. N. R. (2006). *Inorg. Chem.* **45**, 8227–8238.
George, S., Lipstman, S. & Goldberg, I. (2006). *Cryst. Growth Des.* **6**, 2651–2654.
Goldberg, I. (2005). *Chem. Commun.* pp. 1243–1254.
Koner, R. & Goldberg, I. (2008). *Acta Cryst.* C**64**, m264–m266.
Lipstman, S., Muniappan, S., George, S. & Goldberg, I. (2007). *Dalton Trans.* pp. 3273–3281.
Macrae, C. F., Edgington, P. R., McCabe, P., Pidcock, E., Shields, G. P., Taylor, R., Towler, M. & van de Streek, J. (2006). *J. Appl. Cryst.* **39**, 453–457.
Muniappan, S., Lipstman, S., George, S. & Goldberg, I. (2007). *Inorg. Chem.* **46**, 5544–5554.
Nonius (1999). *COLLECT*. Nonius BV, Delft, The Netherlands.
Otwinowski, Z. & Minor, W. (1997). *Methods in Enzymology*, Vol. 276, *Macromolecular Crystallography*, Part A, edited by C. W. Carter Jr & R. M. Sweet, pp. 307–326. New York: Academic Press.
Selman, S. & Eastman, J. F. (1960). *Q. Rev. Chem. Soc.* **14**, 221–235.
Sheldrick, G. M. (2008). *Acta Cryst.* A**64**, 112–122.
Song, J.-L. & Mao, J.-G. (2005). *Chem. Eur. J.* **11**, 1417–1424.